Progress in Computing Applications

DLINE JOURNALS

Print ISSN: 2278 – 6465
Online ISSN: 2278 – 6473

PCA 2026: 15 (1)
https://doi.org/10.6025/pca/2026/15/1/1-17

A Time-to-Failure Aligned Methodological Framework for Sensor Degradation Analysis and Remaining Useful Life Prediction in Industrial IoT Systems

Hathairat Ketmaneechairat
Department of Information and Production Technology Management
College of Industrial Technology
King Mongkut's University of Technology North Bangkok, Thailand
yokehat@gmail.com

ABSTRACT

This study presents a Time to Failure (TTF) aligned methodological framework for analyzing sensor degradation and predicting Remaining Useful Life (RUL) in Industrial Internet of Things (IIoT) systems. Addressing critical challenges of sensor drift and measurement uncertainty, the proposed architecture employs a seven layer pipeline to transform noisy, high frequency telemetry into actionable health indicators. A key innovation is the shift from absolute cycle alignment to TTF aligned trajectory construction, which mitigates survivorship bias and reveals consistent degradation signatures that are otherwise obscured during early operational life. Empirical validation on smart manufacturing datasets (FD001 subset) demonstrates the framework's efficacy: statistical metrics including effect size and Pearson correlation identified sensor_11 and sensor_4 as primary degradation indicators, exhibiting monotonic trends and low inter engine variability. Predictive modeling via Random Forest regression confirmed that TTF aligned features significantly enhance failure prediction accuracy compared to raw sensor inputs. Furthermore, phase aware degradation analysis using change point detection enables robust health state segmentation by distinguishing healthy and transition phases. Static sensors were systematically excluded to reduce computational overhead while preserving prognostic relevance. The framework bridges raw sensor data and reliable decision support, enabling proactive maintenance scheduling that minimizes unplanned downtime and optimizes operational safety in Industry 4.0 environments. Scalability is ensured through containerized inference services, while encryption protocols protect sensitive industrial data. Future work should explore generative models for data recovery and expand validation across heterogeneous fleets to enhance resilience in complex industrial networks, ultimately supporting sustained production quality through data driven prognostics.

Keywords: Time-to-Failure (TTF) Alignment, Sensor Degradation Analysis, Remaining Useful Life (RUL) Prediction, Industrial Internet of Things (IIoT), Predictive Maintenance, Sensor Drift Modeling, Fault Prognosis, Feature Selection, Smart Manufacturing

Received: 19 October 2025, Revised 28 December 2025, Accepted 31 December 2025

1. Introduction

Sensors play a fundamental role in modern industrial systems by enabling the observation and monitoring of physical phenomena such as temperature, pressure, vibration, and chemical composition [1, 2]. By converting variations in physical or chemical properties such as electrical conductivity or hydrogen potential into measurable electrical signals, sensors provide the primary interface between physical processes and digital decision making systems [3, 4, 5].

The rapid evolution of the Industrial Internet of Things (IIoT) has accelerated the deployment of large-scale sensor networks in smart manufacturing environments. In particular, the availability of low cost sensors, including accelerometers, has created new opportunities for precision manufacturing and condition monitoring. Sensor data have become critical inputs for process control, fault diagnosis, and predictive maintenance. While high precision, high cost sensors have traditionally been used for vibration and condition monitoring in industrial settings, the increasing adoption of low cost alternatives necessitates rigorous evaluation of their measurement uncertainty and long term reliability [6].

A key challenge in sensor based monitoring systems is that sensor measurements rarely match the true value of the stimulus being observed. Measurement deviations arise due to intrinsic sensor dynamics, ageing effects, environmental variations, and operational stressors. These deviations, commonly referred to as sensor drift, accumulate over time and can significantly degrade the accuracy and reliability of IIoT based monitoring systems. Understanding and modeling sensor degradation behavior is therefore essential for ensuring dependable fault prognosis and predictive maintenance.

Within the Industry 4.0 paradigm, predictive maintenance has emerged as a strategic approach to maintaining production quality while minimizing unplanned downtime. This paradigm relies heavily on data-driven analysis of IIoT sensor streams to anticipate future system states and proactively schedule maintenance actions [7]. However, achieving reliable predictive maintenance requires robust handling of sensor degradation, data uncertainty, and system level failures, motivating continued research into sensor behavior modeling, fault prognosis, and resilient IIoT architectures.

2. Literature Review

2.1 Sensor Drift and Degradation Modeling

Sensor drift refers to the gradual deviation of sensor outputs from their true values over time. This phenomenon is particularly pronounced in sensors operating in harsh industrial environments or under prolonged operational stress. In gas sensors, drift has been attributed to dynamic processes such as sensor poisoning, ageing, and environmental variations in temperature and pressure, and is commonly modelled using linear or exponential functions [8]. Similar drift behaviors have been observed in pressure sensors, where studies have demonstrated predominantly linear drift patterns and, in rare cases, exponential trends [9, 10, 11].

Comparable modeling approaches have been successfully applied to other sensor types. For instance, exponential drift has been reported in gas sensors [12], whereas linear drift has been observed in pH sensors [13] (Kito) and in silicon based humidity sensors [14] (Islam). Importantly, sensors of the same type often exhibit similar drift functional forms, differing primarily in model parameters rather than in the underlying degradation law [15]. These findings suggest that sensor degradation can be systematically characterized and incorporated into prognostic frameworks.

2.2 Fault Prognosis and Remaining Useful Life Estimation

Fault prognosis aims to estimate the remaining useful life (RUL) of a system or component after a fault is detected, enabling timely maintenance decisions [16]. Prognostic techniques span a wide range of methodologies, including Bayesian estimation, statistical inference, and artificial intelligence based approaches [17, 18].

According to Vachtsevanos et al., fault prognosis methods can be broadly categorized into model based, probability based, and data driven approaches. Model based techniques rely on explicit system models derived from physical principles or historical operational data, ranging from autoregressive integrated moving average (ARIMA) models to advanced neural network architectures. Wu et al. [19] applied ARIMA models to rotor test rig data to predict future system behavior, demonstrating applicability to rotating machinery such as turbines, compressors, and pumps. In contrast, Wu et al. [20] employed recurrent neural networks (RNNs) to capture nonlinear temporal dependencies in multi engine datasets, highlighting the growing role of deep learning in fault prognosis.

2.3 Data-Driven Models and Uncertainty in IIoT Systems

Data-driven approaches leverage historical and real time sensor data to model normal system behavior and detect deviations indicative of faults. These methods encompass statistical techniques [21], stochastic modeling, and machine learning (ML) or deep learning (DL) frameworks. Despite their flexibility, data driven models face challenges arising from noisy measurements, missing data, and sensor degradation [22]. Probabilistic modeling and uncertainty quantification have been proposed as effective means to mitigate these limitations [23].

In IIoT environments, reliability is further compromised by network disruptions and hardware failures, leading to missing or delayed sensor measurements. Cascading failures, in which localized faults propagate across interconnected subsystems, pose a significant threat to system stability. Zheng et al. [24] emphasized that existing cascading failure models often fail to capture the complexity of real industrial scenarios, limiting their practical applicability. To address this gap, they proposed an interdependent network model that explicitly accounts for sensing control data flows, service community structures, and diverse coupling patterns within IIoT systems.

2.4 Generative Models and Data Recovery in IIoT Monitoring

To address data incompleteness and enhance fault detection performance, recent studies have explored the use of generative models in IIoT monitoring systems. Dzaferagic [25] proposed employing generative adversarial networks (GANs) to reconstruct missing sensor measurements, thereby supporting fault detection and classification modules. By generating realistic synthetic data, GAN-based approaches can enhance system robustness under data loss conditions. Extensions of this idea suggest fine tuning generative models based on their downstream impact on diagnostic and prognostic tasks, highlighting the importance of task-aware data augmentation strategies.

3. Architecture Overview

The architecture is structured into seven distinct logical layers, flowing from raw data ingestion to actionable decision support as illustrated in Figure 1. The primary objective is to transform noisy, high frequency sensor data into clear health indicators and reliable failure predictions.

Purpose: To maximize equipment uptime and optimize maintenance schedules through data driven prognostics.

Scope: Covers the end to end lifecycle of sensor data, including ingestion, cleaning, feature engineering, model training, and online deployment.

We set forth the core objectives as following:

Robustness: Handle missing data, outliers, and sensor noise effectively.

Explainability: Provide clear insights into which sensors contribute most to failure prediction.

Scalability: Support multi engine fleets with high volume time series data.

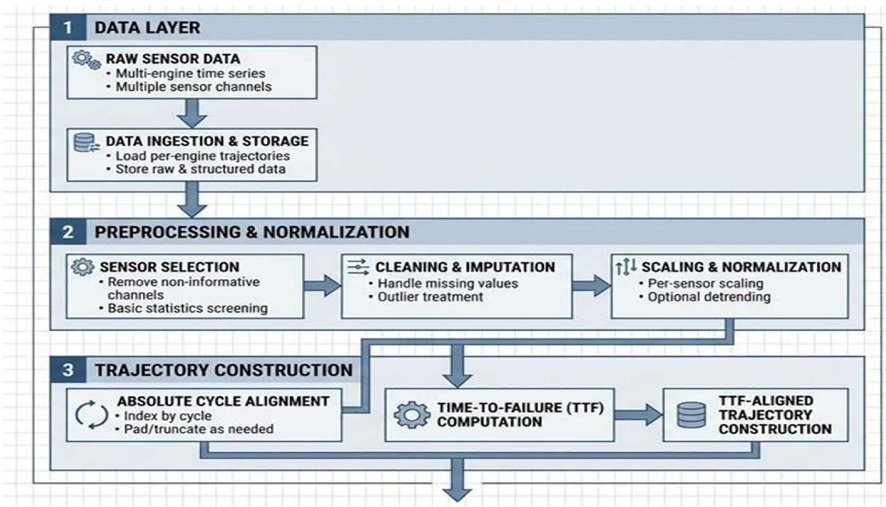

Figure 1. Predictive Maintenance & Remaining Useful Life (RUL) Pipeline

3.1 Layer 1: Data Layer

The foundation of the pipeline, responsible for the reliable collection and storage of raw telemetry.

3.1.2 Raw Sensor Data

The system accepts multi-variate time-series data generated by engine sensors during operation.

Characteristics:

Multi-engine Time Series: Data is organized by unique engine identifiers (Unit ID) and operational cycles (Time Cycles).

Multiple Sensor Channels: Inputs include temperature, pressure, fan speeds, and vibration metrics (e.g., T24, T30, P15, Nf).

Operational Settings: Contextual data such as altitude, mach number, and throttle resolver angle.

Formats: Supports standard industrial formats including CSV, Parquet, and JSON lines for streaming data.

3.2 Data Ingestion & Storage

This component manages the ETL (Extract, Transform, Load) process.

Ingestion Mechanisms:

Batch: Scheduled jobs for historical training data (e.g., nightly dumps).

Stream: Message queues (e.g., Kafka/RabbitMQ) for real-time telemetry.

Storage Architecture:

Raw Zone: Immutable storage (Object Store like S3/Blob) for original sensor logs.

Structured Zone: Columnar databases (e.g., TimescaleDB, InfluxDB) optimized for time-series querying.

3. Layer 2: Preprocessing & Normalization

This layer cleans raw data to ensure model inputs are consistent and statistically valid.

3.3 Sensor Selection

Not all sensors carry degradation signals. Some are constant or purely noise.

Variance Thresholding: Sensors with zero or near-zero variance across the fleet are dropped immediately.

Correlation Analysis: Highly collinear sensors can be removed to mitigate multicollinearity in linear models.

Criteria: A sensor is retained if it shows a statistically significant trend correlated with cycle count.

3.4 Cleaning & Imputation

Ensures data completeness and quality.

Outlier Treatment: Z-score or IQR (Interquartile Range) methods are used to cap extreme values caused by sensor glitches.

Imputation Strategy:

Forward Fill (ffill): Preferred for time-series sensor data to reflect the “last known state”.

Linear Interpolation: Used for short gaps in continuous variables (e.g., temperature).

3.5 Scaling & Normalization

Different sensors have vastly different ranges (e.g., EGT in thousands vs. pressure in tens).

Min-Max Scaling: Maps values to [0, 1]. Useful for Neural Networks.

Z-Score Standardization: Centers data around mean 0 with unit variance. Preferred for regression-based approaches.

Application: Scaling parameters (mean/std) are calculated on the training set only and applied to validation/ test sets to prevent data leakage.

Layer 3: Trajectory Construction

Transforms raw time-steps into meaningful lifecycle trajectories.

Absolute Cycle Alignment

Data is indexed simply by the operational cycle number (1, 2, 3...).

Methodology: Sequences are padded (pre-padding) or truncated to a fixed window length (e.g., the last 50 cycles) for input to models such as LSTMs.

Use Case: Early life behavior analysis where the end-of-life point is unknown.

Time-to-Failure (TTF) Computation

The critical ground-truth label for supervised learning.

RUL Clipping: Often, RUL is clipped at a threshold (e.g., 125 cycles). If TTF > 125, set the target to 125. This teaches the model not to predict failure too early when the engine is healthy.

TTF-aligned Trajectory Construction

Re-indexes data backwards from the failure point (Failure = 0).

Benefit: Aligns all engines at their failure point, making degradation patterns (e.g., exponential rise in temperature) clearly visible and comparable across the fleet.

Windowing: Creates sliding windows of sensor data (e.g., window size 30) associated with a specific target RUL.

3.6 Data Flow & Integration

The architecture relies on a continuous data flow with strategic feedback loops.

Metric	Description	Utility
Monotonicity	Measures whether the trend is consistently strictly increasing or decreasing	High monotonicity implies easy to model degradation.
Trendability	Correlation between sensor value and time index.	Ensures the sensor changes over time
Prognosability	Variance of sensor value at failure point.	Low failure variance is preferred (consistent failure mode).

Table 1. Sensor Metric

Feedback Loop: The Sensor Health Scores from Layer 6 are fed back into Layer 5. This allows the RUL model to know not only the raw sensor values but also how “abnormal” they are relative to a healthy baseline.

3.7 Implementation Considerations

Technology Stack

Languages: Python (Pandas, NumPy, Scikit-Learn, PyTorch/TensorFlow).

Data Processing: Apache Spark (for large historical datasets).

Orchestration: Apache Airflow or Kubeflow Pipelines.

Visualization: Grafana or Streamlit.

Scalability & Performance

Horizontal Scaling: Inference services are containerized (Docker/Kubernetes) to scale with the number of monitored engines.

Caching: Redis is used to cache recent feature windows to avoid re-computing history for every new data point.

Security & Compliance

Encryption: TLS 1.3 for data in transit; AES-256 for data at rest.

Access Control: Role-Based Access Control (RBAC) restricts access to raw sensor data versus aggregated reports.

3.8 Common Challenges & Solutions (Table 2)

Challenge	Solution
Model Drift	Continuous monitoring of prediction error distributions. Periodic retraining on new failure data.
Data Quality	Strict schema validation at ingestion. Automated alerts for sensor dropouts.
Imbalanced Data	Failure data is rare. Techniques such as oversampling or synthetic data generation (e.g., GANs) can be explored.

Table 2. Common Challenges

3.9 Architecture Summary

This architecture provides a robust framework for predictive maintenance. By combining traditional physics-based feature engineering with modern deep learning and generative anomaly detection, the system delivers accurate RUL estimates that directly translate to operational savings and improved safety.

4. Methodology and Data Processing

This section describes the data preprocessing, trajectory alignment, and degradation analysis procedures adopted to characterise sensor behaviour and extract reliable degradation signatures from multivariate time-series data. The methodology is designed to ensure comparability across units with heterogeneous operating histories while preserving physically meaningful degradation dynamics.

4.1 Data Preprocessing

4.1.1 Sensor Selection and Normalization

Prior to analysis, sensor channels were screened to remove non informative or quasi constant signals that do not contribute meaningful degradation information. Sensors exhibiting negligible variance across all operating cycles were excluded in accordance with established guidelines for condition monitoring and prognostics datasets.

To mitigate the effects of operating condition variability, each retained sensor was normalised prior to trajectory analysis. Specifically, sensor values were standardized using either z-score normalization within each operating regime or min max scaling on a per sensor basis. This normalization step prevents shifts in operating conditions from being misinterpreted as degradation trends and ensures that subsequent analyses reflect intrinsic health evolution rather than regime dependent offsets.

4.1.2 Engine-wise Segmentation

The dataset consists of multiple independent engine units, each operating until failure. For each engine, the complete multivariate sensor time series was extracted from the initial operational cycle up to the failure cycle. Let T_i denote the failure cycle of engine i; all sensor trajectories for that engine are defined over the interval $t=1,\ldots,T_i$. This engine-wise segmentation preserves unit specific temporal dynamics and enables subsequent alignment strategies.

4.2 Absolute Cycle Index–Aligned Trajectory Analysis

4.2.1 Trajectory Construction

In the first analysis setting, sensor trajectories were aligned using the absolute cycle index. All engines were synchronized at cycle t=1, corresponding to the start of operation, and sensor values were aggregated across engines at each cycle index. To accommodate varying lifetimes, longer trajectories were truncated to a common horizon, while shorter sequences were padded with missing values. Aggregation statistics were computed while ignoring missing entries.

4.2.2 Analysis Procedure

For each sensor, individual engine trajectories were visualized as light lines, overlaid with the population mean trajectory and a variance band corresponding to ± one standard deviation. This representation enables simultaneous inspection of unit-level variability and population-level trends.

4.2.3 Interpretation

Absolute cycle alignment highlights early life stationarity and late life divergence across engines, revealing sensors whose degradation signatures emerge only after extended operation. However, because engines fail at different cycle counts, late-cycle aggregation is affected by survivorship bias, which limits the interpretability of absolute alignment in failure centric analyses.

4.3 Time-to-Failure (TTF)–Aligned Trajectory Analysis

4.3.1 Time-to-Failure Transformation

To obtain a failure centric view of degradation, sensor trajectories were re-parameterized in terms of time-to-failure (TTF). For each engine i, TTF was defined as

$$\mathsf{TTF}_i(t) = T_i - t,$$

such that failure occurs at TTF=0 and earlier operational stages correspond to larger TTF values. This transformation effectively reverses the temporal axis and aligns all engines at the failure event.

4.3.2 Alignment and Aggregation

All engines were aligned at , and a common TTF window corresponding to the final portion of life was selected. Sensor values were aggregated across engines at each TTF index to compute mean degradation trajectories and associated confidence bands.

4.3.3 Analysis Outputs

For each sensor, the following quantities were derived as functions of TTF: (*i*) mean degradation trajectory, (*ii*) variability across engines, and (*iii*) first and second order temporal derivatives capturing degradation rate and acceleration. These outputs reveal degradation onset, late stage collapse behavior, and linear versus nonlinear degradation patterns.

4.3.4 Interpretation

TTF-aligned trajectories substantially reduce inter-engine variability and expose consistent degradation signatures that are otherwise obscured under absolute cycle alignment. Sensors that appear weakly informative during early life often become sharply discriminative near failure, underscoring the importance of TTF alignment for prognostic modeling.

4.4 Piecewise Degradation Phase Identification

4.4.1 Phase Definition

To further characterize degradation evolution, sensor trajectories were partitioned into distinct degradation phases. The Healthy Phase is characterized by low variance, near-zero trend slope, and fluctuations around a steady mean. The Transition Phase corresponds to the onset of persistent trends, increasing variance, and monotonic degradation behavior.

Operationally, phase boundaries were defined using statistical change point detection criteria rather than fixed thresholds, enabling adaptive identification across engines and sensors.

4.4.2 Change-Point Detection

Change-point detection methods were applied either directly to individual sensor trajectories or to a derived health indicator. Techniques such as cumulative sum (CUSUM), Bayesian change point detection, and segmentation based methods were used to identify the cycle at which degradation transitions from healthy to deteriorating behavior.

The detected change point separates the healthy phase from the transition phase, providing a principled basis for phase-aware modeling.

4.4.3 Health Indicator–Based Phase Detection

To improve robustness, a composite health indicator was constructed using multi-sensor fusion techniques such as principal component analysis or latent representations learned via autoencoders. Change-point detection was then applied to the health indicator rather than raw sensor signals. This approach suppresses sensor level noise, captures correlated degradation patterns, and yields clearer phase separation.

4.5 Visualization Strategy

To support interpretability and reproducibility, three primary visualization types were employed: (i) absolute cycle aligned trajectories for selected sensors, (ii) TTF-aligned degradation curves with confidence bands, and (iii) piecewise trajectories highlighting healthy and transition phases with detected change points. These visualizations provide complementary perspectives on degradation behavior and are critical for conveying results in a publication setting.

4.6 Summary of Methodological Insights

The proposed methodology systematically progresses from raw sensor preprocessing to failure-centric trajectory alignment and phase-aware degradation analysis. Absolute cycle alignment captures population-level variability, whereas TTF alignment reveals intrinsic degradation dynamics. The healthy phase predominates in early life and masks signatures of failure, whereas the transition phase contains the most prognostic information. Incorporating phase awareness into modeling is therefore expected to improve the accuracy and stability of remaining useful life predictions.

5. Dataset

The data source contains a dataset designed for Industrial IoT (IIoT) edge computing applications in smart manufacturing. The dataset includes real-time sensor data, edge processing times, maintenance statuses, and

Fuzzy PID controller outputs, enabling research on predictive maintenance and autonomous decision making.

5.1 Dataset Contents

The dataset comprises multivariate time series records collected from an Industrial Internet of Things (IIoT) enabled smart manufacturing environment. Each record is indexed by timestamps and sensor identifiers, enabling temporal alignment and cross sensor analysis. The measurements include key physical process variables namely, temperature (°C), pressure (kPa), and vibration frequency (Hz) that capture the equipment's operational and mechanical state. In addition to process-level variables, the dataset includes system-level performance metrics, such as network latency (ms) and edge processing time (ms), which reflect communication and computation overheads in edge-based deployments. The output of a Fuzzy Proportional Integral Derivative (PID) controller is also provided as a normalized adaptive control signal in the range [0, 1]. Equipment health is annotated using discrete maintenance status labels (Normal, Warning, and Failure). Finally, a binary failure indicator is included as the target variable, with 1 denoting failure and 0 denoting normal operation, facilitating supervised learning and predictive maintenance studies**.**

5.2 Descriptive Analysis of Sensor Degradation and Failure Indicators

This section presents a comprehensive analysis of sensor behavior under time to failure (TTF) alignment, with the objective of identifying robust degradation indicators and validating their relevance for failure prediction and remaining useful life (RUL) modeling. All results are derived from the FD001 subset, in which sensor trajectories are aligned relative to the failure, enabling a consistent comparison across units.

5.3 Univariate Degradation Strength Across Sensors

Sensor	**Mean_Far**	**Mean_Near**	**Delta_Mean**	**Effect_Size**
sensor_11	47.8024	48.1798	0.3774	2.864965
sensor_4	1418.396	1430.873	12.4773	2.828226
sensor_12	520.6808	519.6715	-1.0093	-2.58076
sensor_7	552.5567	551.3617	-1.195	-2.40517
sensor_20	38.6537	38.4022	-0.2515	-2.29026
sensor_15	8.474883	8.524108	0.049225	2.27957
sensor_21	23.20635	23.05339	-0.15296	-2.24864
sensor_2	643.0654	643.7218	0.6564	2.050686
sensor_17	394.52	396.6	2.08	1.960119
sensor_3	1595.964	1602.499	6.5348	1.547148
sensor_13	2388.152	2388.252	0.1001	1.458318
sensor_8	2388.152	2388.246	0.0947	1.400375
sensor_9	9077.69	9099.36	21.6693	0.479514
sensor_14	8152.754	8168.125	15.3708	0.377148
sensor_10	1.3	1.3	0	0
sensor_6	21.61	21.61	0	0
sensor_5	14.62	14.62	0	0
sensor_16	0.03	0.03	0	0
sensor_18	2388	2388	0	0
sensor_19	100	100	0	0
sensor_1	518.67	518.67	0	0

Table 3. Top Sensors Ranked by Effect Size

Table 3 reports the top sensors ranked by absolute effect size, computed as the normalized difference between mean sensor values at a distant operating point (TTF = 30) and at failure (TTF = 0). This metric captures not only the magnitude of change but also its consistency across engines by accounting for pooled variability.

The results indicate that sensor_11 and sensor_4 exhibit the strongest degradation signatures, with effect sizes exceeding 2.8. Although the absolute change in sensor_11 is small, its exceptionally low variance yields a highly consistent, statistically significant indicator of degradation. In contrast, sensor_4 exhibits both substantial absolute drift and high consistency, making it a well-known degradation sensor in the FD001 dataset.

Several sensors, including sensor_12, sensor_7, sensor_20, and sensor_21, demonstrate negative effect sizes, indicating systematic decreases as failure approaches. The presence of both increasing and decreasing trends highlights the heterogeneous nature of degradation mechanisms captured by different sensors. Importantly, sensors with near-zero effect sizes (e.g., sensor_5, sensor_6, sensor_10, sensor_16, sensor_18, sensor_19) remain effectively constant over the degradation horizon, suggesting limited diagnostic value and justifying their exclusion in downstream modeling.

Overall, Table 1 clearly distinguishes informative degradation sensors from quasi-static or redundant channels, providing a principled basis for sensor selection.

5.4 Correlation Between Sensor Values and Time-to-Failure

To complement the effect size analysis, sensor relevance was further examined through Pearson correlations with TTF, summarised in Table Y. Strong negative correlations indicate sensors whose values increase as failure approaches, whereas positive correlations indicate decreasing trends.

Consistent with the effect-size ranking, sensor_11, sensor_4, sensor_15, sensor_2, sensor_17, and sensor_3 exhibit strong negative correlations with TTF, indicating a monotonic upward drift toward failure. Conversely, sensor_12, sensor_7, sensor_21, and sensor_20 show strong positive correlations, reflecting consistent downward trajectories.

The moderate to high magnitude of these correlations (approximately 0.58–0.70 in absolute value) is notable given the inherently noisy nature of real-world sensor data. These results reinforce the interpretation that the identified sensors are not merely drifting on average but are closely tied to the degradation process captured by TTF alignment.

5.5 Per-Engine Trend Consistency

While global statistics are informative, degradation indicators must also be consistent at the individual engine level. To assess this, per-engine linear regressions of sensor value versus TTF were performed, and the resulting slope distributions are summarized in Table 4.

Sensors such as sensor_4 and sensor_11 exhibit tightly clustered slope distributions with consistent signs across engines, indicating highly reliable degradation behavior. Sensor_11, in particular, exhibits very small absolute slopes due to its scale but shows extremely low inter-engine variability, making it a stable indicator across the fleet.

sensor	corr_TTF	avg_slope_per_TTF	std_slope_per_TTF
sensor_11	-0.6962281014553727	-0.0033760817309102338	0.0008999686096815563
sensor_4	-0.6789482333860427	-0.11091786196841595	0.026952400010780513
sensor_12	0.6719831036133275	0.009034209961582754	0.0027415488655236626
sensor_7	0.6572226620546537	0.010547780362040462	0.003032971355604084
sensor_15	-0.6426670441974635	-0.0004376785066365394	0.00010761326935908209
sensor_21	0.6356620421802941	0.001249195406762645	0.0003061227723120686
sensor_20	0.6294284994377553	0.0020844646813577773	0.0005213211541640201
sensor_2	-0.6064839743785985	-0.005488195133038601	0.0014140444483167975
sensor_17	-0.6061535537829565	-0.017017343702970585	0.003672555873833868
sensor_3	-0.5845203909176561	-0.0651425657263318	0.015000248465346672

Table 4. Slope Distributions

Other sensors, including sensor_12 and sensor_7, also display coherent per-engine trends, albeit with slightly higher variability. Sensors with large slope variance or mixed slope signs are less reliable as global indicators and are therefore less suitable for generalised RUL modelling.

This per-engine analysis confirms that the strongest sensors identified earlier are not artefacts of aggregation but reflect genuine, repeatable degradation dynamics.

5.6 Predictive Validation via Feature Importance

To evaluate the practical utility of the sensors, a Random Forest regressor was trained to predict TTF using all sensor channels. Table W reports the resulting feature importance scores.

The dominance of sensor_11, which accounts for approximately 40% of the total importance, underscores its critical role in predicting degradation state. Sensor_4 emerges as the second most important feature, followed by a cluster of sensors previously identified as informative in effect-size and correlation analyses (sensor_12, sensor_7, sensor_21, sensor_15, sensor_3, sensor_2).

Interestingly, sensor_9 and sensor_14 appear among the top features despite more modest univariate correlations, suggesting that nonlinear interactions captured by the ensemble model can extract additional information not evident in linear analyses alone. The strong overlap between univariate metrics and model-based importance provides compelling validation of the identified sensor set.

5.7 Aggregated Degradation Trajectories

Figure 2 illustrates the mean ± standard deviation of selected top sensors as functions of TTF, computed over binned intervals. These plots provide an intuitive visualization of degradation behavior.

Sensor_11 and sensor_4 exhibit smooth, near-linear decreases in TTF, with narrow variance bands, indicating low noise and high predictability. In contrast, sensor_12 and sensor_7 show clear downward trends, again with relatively tight dispersion. The monotonicity and smoothness of these curves are characteristic of high-quality degradation indicators and are particularly suitable for phase detection and RUL regression.

Notably, the variance tends to increase slightly at higher TTF values, reflecting greater operational diversity during early life, and then converges near failure—a pattern commonly observed in degradation processes.

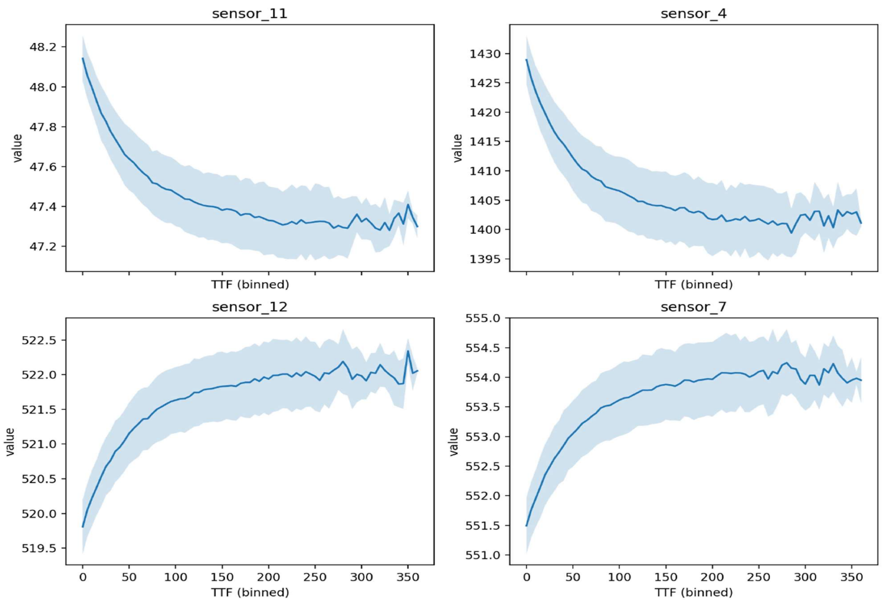

Figure 2. Aggregated Degradation Trajectories

5.8 Summary of Findings

Taken together, the analyses presented in Tables X–W and Figures X demonstrate that a subset of sensors—most prominently sensor_11, sensor_4, sensor_12, sensor_7, sensor_21, sensor_15, sensor_2, sensor_3, and sensor_17—consistently encode degradation information across multiple statistical perspectives. These sensors exhibit large effect sizes, strong correlations with TTF, consistent per-engine trends, and significant predictive importance.

The convergence of evidence across univariate, multivariate, and model based analyses provides strong validation of their relevance and supports their use in subsequent degradation modeling, health state segmentation, and RUL prediction frameworks.

6. Conclusion

This study establishes a robust Time-to-Failure (TTF) aligned methodological framework for analyzing sensor degradation and predicting Remaining Useful Life (RUL) within Industrial Internet of Things (IIoT) systems. To address sensor drift and uncertainty, the proposed architecture transforms noisy telemetry into actionable health indicators via a seven-layer pipeline. By shifting from absolute cycle alignment to TTF-aligned trajectory construction, the methodology mitigates survivorship bias and exposes consistent degradation signatures that would otherwise remain obscured during early operational life, ensuring that patterns become visible across the fleet.

An empirical analysis of smart manufacturing datasets validated the framework's efficacy. Statistical metrics, including effect sizes and Pearson correlations, identified sensor_11 and sensor_4 as primary indicators of degradation. These sensors demonstrated monotonic trends and low inter engine variability, proving essential for accurate prognostics. Furthermore, predictive modeling via Random Forest regression confirmed that TTF-aligned features significantly enhance failure prediction accuracy compared to raw data inputs. The integration of phase aware degradation analysis further refines health state segmentation by distinguishing between healthy and transition phases via change point detection. Conversely, static sensors were excluded to reduce computational overhead.

Ultimately, this research bridges the gap between raw sensor data and reliable decision support. By ensuring robustness against data uncertainty and highlighting specific degradation dynamics, the framework enables proactive maintenance scheduling. This approach minimizes unplanned downtime and optimizes operational safety in Industry 4.0 environments. Scalability is ensured via containerized inference. Security protocols, such as encryption, further protect sensitive industrial data. Future implementations should explore integrating generative models for data recovery and expanding validation across heterogeneous fleets to enhance resilience in complex industrial networks, ensuring sustained production quality and minimizing operational costs through data driven prognostics.

References

[1] Wilson, J. S. (2004). Sensor technology handbook. *Elsevier*.

[2] Algamili, A. S., Khir, M. H. M., Dennis, J. O., Ahmed, A. Y., Alabsi, S. S., Ba Hashwan, S. S., Junaid, M. M. (2021). A review of actuation and sensing mechanisms in MEMS-based sensor devices. *Nanoscale Research Letters*, 16, 1-21.

[3] Basuwaqi, A. M., Khir, M. M., Ahmed, A. Y., Rabih, A. A., Mian, M. U., & Dennis, J. O. (2017). Effects of frequency and voltage on the output of CMOS-MEMS device. *In* 2017 IEEE Asia Pacific Conference on Postgraduate Research in Microelectronics and Electronics (PrimeAsia) (p. 49-52). *IEEE*.

[4] Su, Y., Ma, C., Chen, J., Wu, H., Luo, W., Peng, Y., Li, H. (2020). Printable, highly sensitive flexible temperature sensors for human body temperature monitoring: a review. *Nanoscale Research Letters*, 15, 1-34.

[5] Trung, Thanh., Thai, Phuc, Do., Benoit, Iung., Paolo, Gardoni. (2025). Impact of Sensor Degradation on Measurement Uncertainty in Prognostics and Maintenance Decision-Making: State of the Art and Challenges. *International Journal of Prognostics and Health Management*, 2025, 16 (4).

[6] Iqbal, Ali., Mian, Naeem., S., Longstaff, Andrew., Fletcher, Simon. (2022). Performance Evaluation of Low-Cost Vibration Sensors in Industrial IoT Applications, *International Journal of Automation Technology*. VL - 16 (3) p. 329 - 339.

[7] Dall'Ora, N., Centomo, S., Fummi, F. (2009). Industrial-IoT Data Analysis Exploiting Electronic Design Automation Techniques, *In*: *2019 IEEE 8th International Workshop on Advances in Sensors and Interfaces (IWASI), Otranto, Italy,* 2019, p. 103-109.

[8] Flitti, F., Aicha, F., Guo, B., Bermak, A. (2008). A Robust and Low-Complexity Gas Recognition Technique for On-Chip Tin-Oxide Gas Sensor Array. *J. Sens.* 2008, 2008, 465209.

[9] Matsumoto, H., Araki, E. (2021). Drift Characteristics of DONET Pressure Sensors Determined From In-Situ and Experimental Measurements. *Front. Earth Sci.* 8, 600966.

[10] Watts, R., Kontoyiannis, H. (1990). Deep-ocean bottom pressure measurement: Drift removal and performance. *J. Atmos. Ocean. Technol.* 7, 296–306.

[11] Polster, A., Fabian, M., Villinger, H. (2009). Effective resolution and drift of Paroscientific pressure sensors derived from long-term seafloor measurements. Geochem. *Geophys. Geosyst.* 2009, 10.

[12] Nelli, P., Faglia, G., Sberveglieri, G., Cereda, E., Gabetta, G., Dieguez, A., Romano-Rodriguez, A., Morante, J. (2000). The aging effect on SnO2–Au thin film sensors: *Electrical and structural characterization. Thin Solid Film.* 2000, 371, 249–253.

[13] Kito, O., Christian, T., Marco, K., Juan, P. C., Kris, V. (2019). Characterizing long-term wear and tear of ion-selective pH sensors. *Water Sci. Technol.* 2019, 80, 541–550.

[14] Islam, T., Saha, H. (2007). Study of long-term drift of a porous silicon humidity sensor and its compensation using ANN technique. *Sens. Actuators A Phys.* 2007, 133, 472–479.

[15] Kajmakovic, A., Diwold, K., Römer, K., Pestana, J., Kajtazovic, N. (2022). Degradation Detection in a Redundant Sensor Architecture. *Sensors* 2022, 22, 4649.

[16] Vachtsevanos, G., Wang, P. (2001). Fault prognosis using dynamic wavelet neural networks. *In:* Proceedings of the 2001 IEEE Autotestcon Proceedings, *IEEE Systems Readiness Technology Conference,* (Cat. No. 01CH37237), Valley Forge, PA, USA, 20–23 August 2001 p. 857–870.

[17] Vachtsevanos, G. J., Vachtsevanos, G. J. (2006). Intelligent Fault Diagnosis and Prognosis for Engineering Systems; *Wiley Online Library: Hoboken, NJ, USA*, 2006; Volume 456.

[18] Rathore, S. S., Kumar, S. (2019). A study on software fault prediction techniques. *Artif. Intell. Rev.* 2019, 51, 255–327.

[19] Wu, W., Hu, J., Zhang, J. (2007). Prognostics of Machine Health Condition using an Improved ARIMA-based Prediction method. *In*: Proceedings of the 2007 2nd *IEEE Conference on Industrial Electronics and Applications, Harbin, China,* 23–25 May p. 1062–1067.

[20] Wu, Q., Ding, K., Huang, B. (2020). Approach for fault prognosis using a recurrent neural network. *J. Intell. Manuf.* 31, 1621–1633.

[21] Carden, E. P., Fanning, P. (2004). Vibration-Based Condition Monitoring: A Review. *Struct. Health Monit.* 3 (4), 355–377.

[22] Dai, X., Gao, Z. (2013). From Model, Signal to Knowledge: A Data-Driven Perspective of Fault Detection and Diagnosis. *IEEE Trans. Ind. Inf.* 9 (4), 2226–2238.

[23] Ovidiu, Vermesan. (2022). An Intelligent Real-Time Edge Processing Maintenance System for Industrial Manufacturing, Control, and Diagnostic, *Front. Chem. Eng.*, 01 July 2022. Sec. *Computational Methods in Chemical Engineering*. Volume 4 - 2022

[24] Zheng, D., Fu, X., Liu, X., Xing, L., Peng, R. (2025). Modeling and Analysis of Cascading Failures in Industrial Internet of Things Considering Sensing-Control Flow and Service Community, *IEEE Transactions on Reliability,* vol. 74, no. 2, p. 2723-2737, June.

[25] Dzaferagic, M., Marchetti, N., Macaluso, I. (2022). Fault Detection and Classification in Industrial IoT in Case of Missing Sensor Data, *IEEE Internet of Things Journal,* vol. 9 (11), p. 8892-8900, 1 June 1.